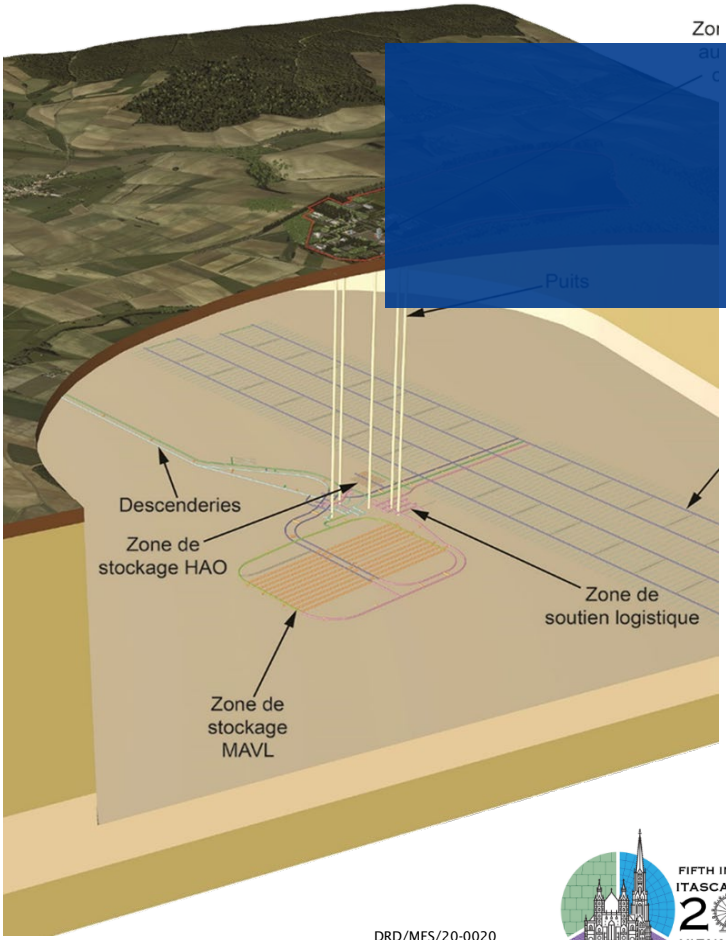

3D ANISOTROPIC MODELLING OF DEEP DRIFTS AT THE MEUSE/HAUTE-MARNE URL

Mountaka SOULEY[1], **Minh Ngoc VU**[2], Gilles ARMAND[2]

[1]French national institute for industrial environment and risks (Ineris), France
[2]French national radioactive waste management agency (Andra), France

Fifth International Itasca Symposium

16 – 21 February 2020 – Vienna (Austria)

Meuse/Haute Marne Underground Research Laboratory (Andra URL)

Andra started in 2000 to build the URL for research on the feasibility of a possible deep geological repository (Cigéo project)

- Scientific and technological program to
  - Characterize the confining properties of the claystone COx
  - Test and Demonstrate the feasibility of the repository components
  - Optimize concept/design of the different components

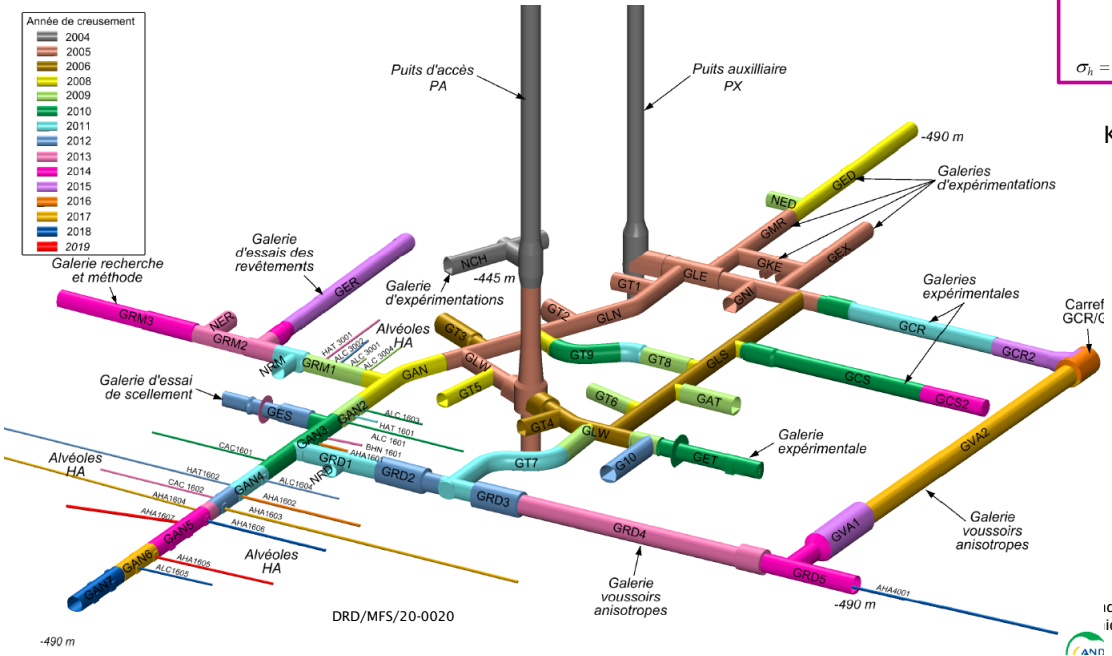

DRD/MFS/20-0020

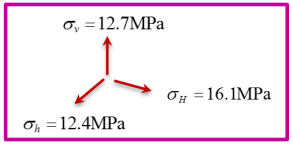

Key numbers

- ~2 km of drifts
- ~8000 m of core drillings
- ~11 500 sensors
- ~40 experiments

Behavior of drifts within the Andra URL

In-situ observations – Excavation induced fractured zone

- Anisotropic induced fractured zone: extension is proportional to the drift diameter
- Fractured zone plays an important role for hydromechanical responses
  - Anisotropic convergence
  - Anisotropic pore pressure field around drift

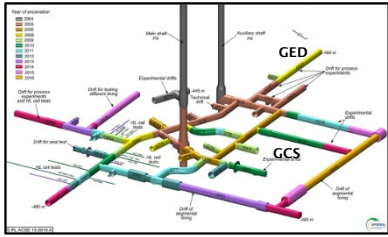

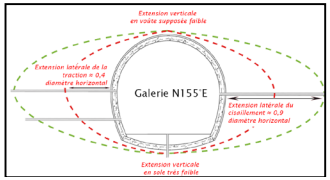

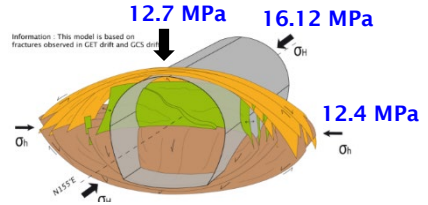

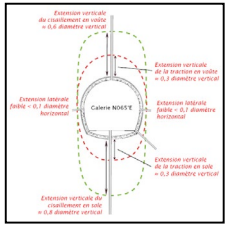

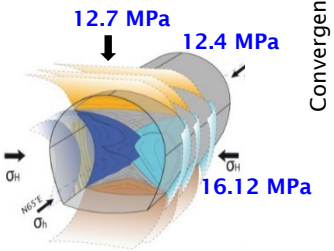

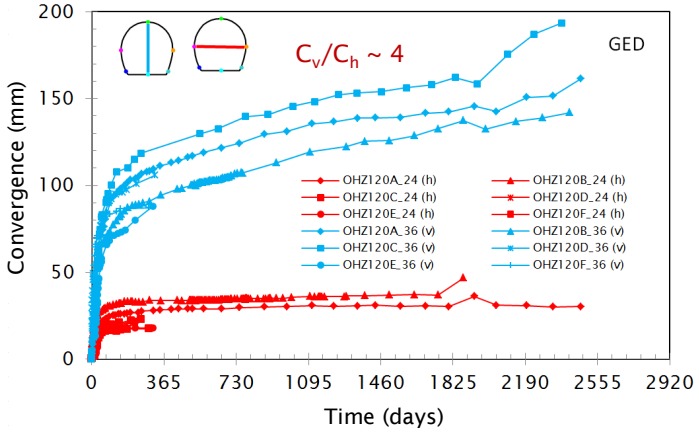

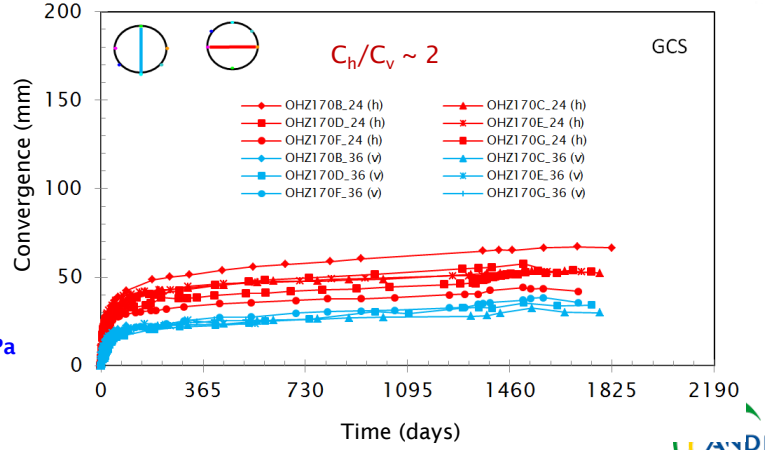

Behavior of drifts within the Andra URL

Overview of modeling– Excavation induced fractured zone

- ~15 teams have worked on the modeling of excavation induced damage around drifts in Andra URL
  - Approches continuum mechanic/discrete/hybrid elements
    - Differents constitutive models: elasto-damage, elasto-visco-plastic, …
    - Hydro-mechanical coupling
    - Necessity of anisotropic stiffness and strength
    - Advanced numerical modeling: non-local, second gradient regularization, far-field methods

2D representation

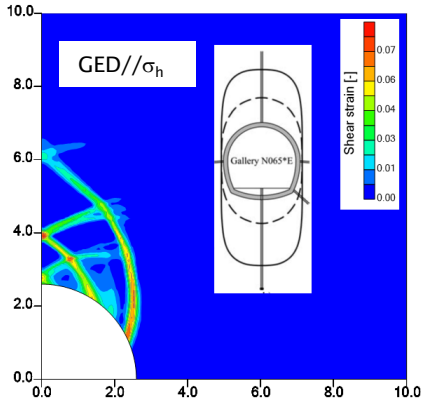

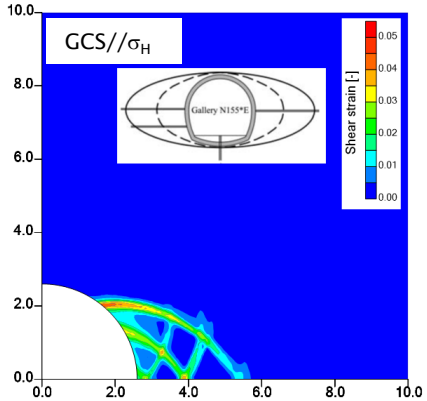

Non-local anisotropic elasto-visco-plastic model (Manica et al 2018)

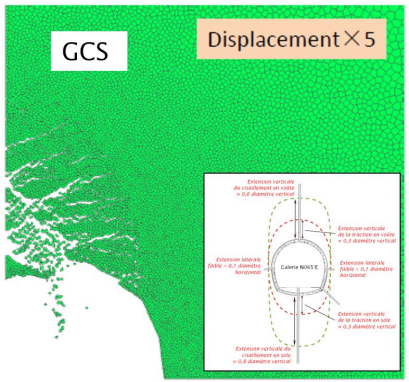

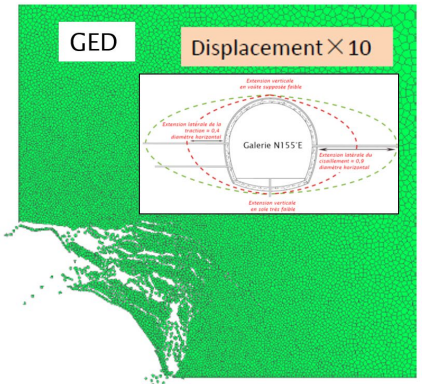

Extended rigid block spring method (Yao et al 2017)

Anisotropic behavior of geometerials

- Sedimentary rock exhibits tranverse isotropy
  - Mechanical behavior is a directional dependency: stifness, strengths
    - Maximum strength generally corresponds to the direction perpendicular to bending
    - Minimum strength reached when θ between 30 to 60° with respect to bending
- 3 main class of models for anisotropic geomaterials
  - Empirical description based on the variation of cohesion and/or friction
  - Models based on plasticity and/or damage theory formulated in the framework of the thermodynamics of irreversible processes
  - Discontinuous Weakness Plane (DWP) concept or « Ubiquitous joints »
    - Description of the physical mechanism related to the failure precess
    - Extension of Griffith theory
- Purposes: 3D modeling for induced anisotropy of excavation induced damage around drifts in MHM-URL by a coupling between ubiquitous joints and elasto-plastic matrix implemented in FLAC3D
  - Induced anisotropy is due to
    - Failure of rock matrix based on elastoplastic approach
    - Failure of weakness planes occurs in post peak behavior of rock matrix

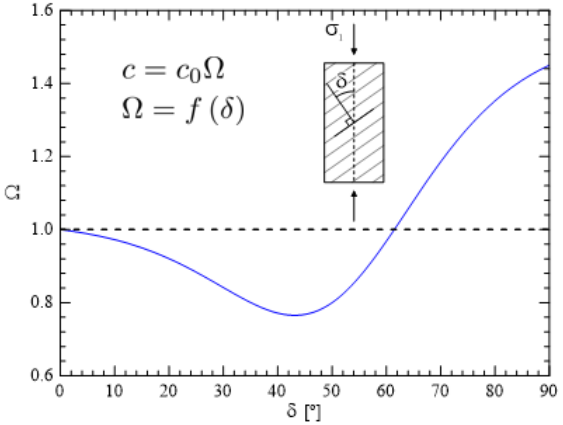

(Manica et al 2018)

Constitutive model
Rock matrix

- Shear yield functions (initiation, peak, residual) (Souley et al 2017)
  - Hoek-Brown criteria formulated by three stress invariant (p,q,θ)
  - Shear strength is lower in extension stress path than in compression stress path
  - Strain hardening (in pre-peak) and strain softening (in post-peak): Parameters A (friction angle) and B (cohesion) = second order function of γ plastic distorsion
  - Shear strength depends on confining stress → brittle – ductile transition

$$F_s^{\,m} = \frac{4}{3}\frac{cos^2\theta}{A}q^2 + \left(\frac{cos\,\theta}{\sqrt{3}} - \frac{sin\,\theta}{3}\right)q + p - \frac{B}{A} \qquad A = \sigma_c\, m \text{ et } B = s\,\sigma_c{}^2$$

- Shear plastic potential

$$G_s^{\,m} = \left(\frac{\cos\theta}{\sqrt{3}} - t_c\frac{\sin\theta}{3}\right)q + \beta(\gamma)p$$

$$\beta(\gamma) = \beta_m - (\beta_m - \beta_0)e^{-b_\beta \gamma}$$

- Tensile yield function $F_t^{\,m} = \sigma - \sigma_t$

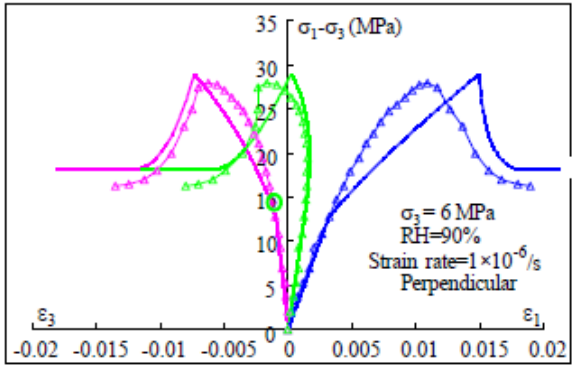

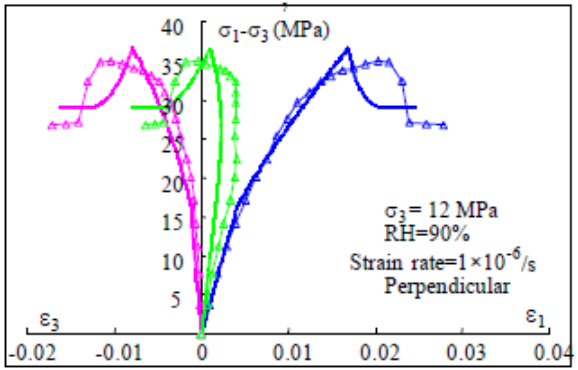

Constitutive model
Weakness plane

- Induced fractures represented by weakness planes based on the notation of ubiquituous joints within the rock matrix
- Weakness plane orientation: based on fracture mechanic on brittle material
  - Extension fracture: tensile fracture ($\sigma_3>\sigma_t$) and longitudial splitting fracture (weak σ_3 or $\sigma_3=0$) → weakness plane $\perp \sigma_3$
  - Shear fracture occurs in triaixal compressive stress path: conjugate planes
    - Direction of σ_3
    - normal to $(45° - \Psi wp/2)$ with respect to the axial load direction
    - normal to $\pm(45° - \Psi wp/2)$ with respect to the axial load direction
- Prefectly elastoplastic Mohr-Coulomb
  - Yield functions and plastic potential written in the local coordinate system

$$\begin{cases} F_s^{wp} = \tau + \sigma_{nn} \tan\phi_{wp} - C_{wp} \\ F_t^{wp} = \sigma_{nn} - \sigma_{wp}^t \end{cases} \qquad \begin{cases} G_s^{wp} = \tau + \sigma_{nn} \tan\psi_{wp} \\ G_t^{wp} = \sigma_{nn} \end{cases}$$

  - Dilatancy rate

$$tg(\psi) = \begin{cases} tg(\psi_{wp}) & si\ \gamma_{wp} \le (\gamma^{ult} - \gamma^{pic}) \\ tg(\psi_{wp}) e^{\left(1 - \gamma_{wp}/(\gamma^{ult} - \gamma^{pic})\right)} & \gamma_{wp} > (\gamma^{ult} - \gamma^{pic}) \end{cases}$$

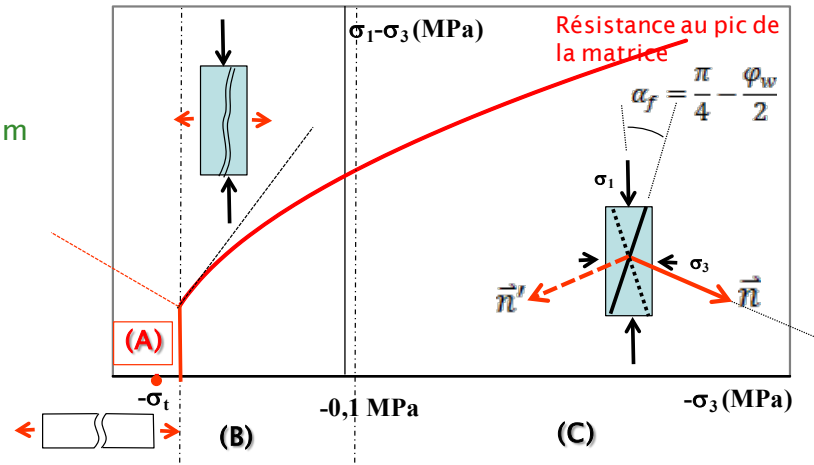

Implementation in FLAC3D via UDM
Algorithm

- Input $\Delta\varepsilon$, σ^{old}, κ^{old}
- Computation of the first approximation stress tensor σ^{i} (p^{i},q^{i},θ^{i})
- Verification of yield function for rock matrix
  - $F^{m}(p^{i},q^{i},\theta^{i}) \leq 0$ the current stress $\sigma^{0} = \sigma^{i}$
  - $F^{m}(p^{i},q^{i},\theta^{i}) > 0$ make correction to get σ^{0}
- Writting σ^{0} in the local system of weakness plan σ'^{0} (σ'_{n},τ')
- Verification of yield function for weakness plan
  - $F^{wp}(\sigma'_{n},\tau') \leq 0$ the current stress $\sigma'^{n} = \sigma'^{0}$
  - $F^{wp}(\sigma'_{n},\tau') > 0$ make correction to get σ'^{n}
- Back to global system (x,y,z) σ^{new}
- Update internal plastic variable κ^{new}
- Next step

Simulation triaxial test without WP

Stress-strain curves

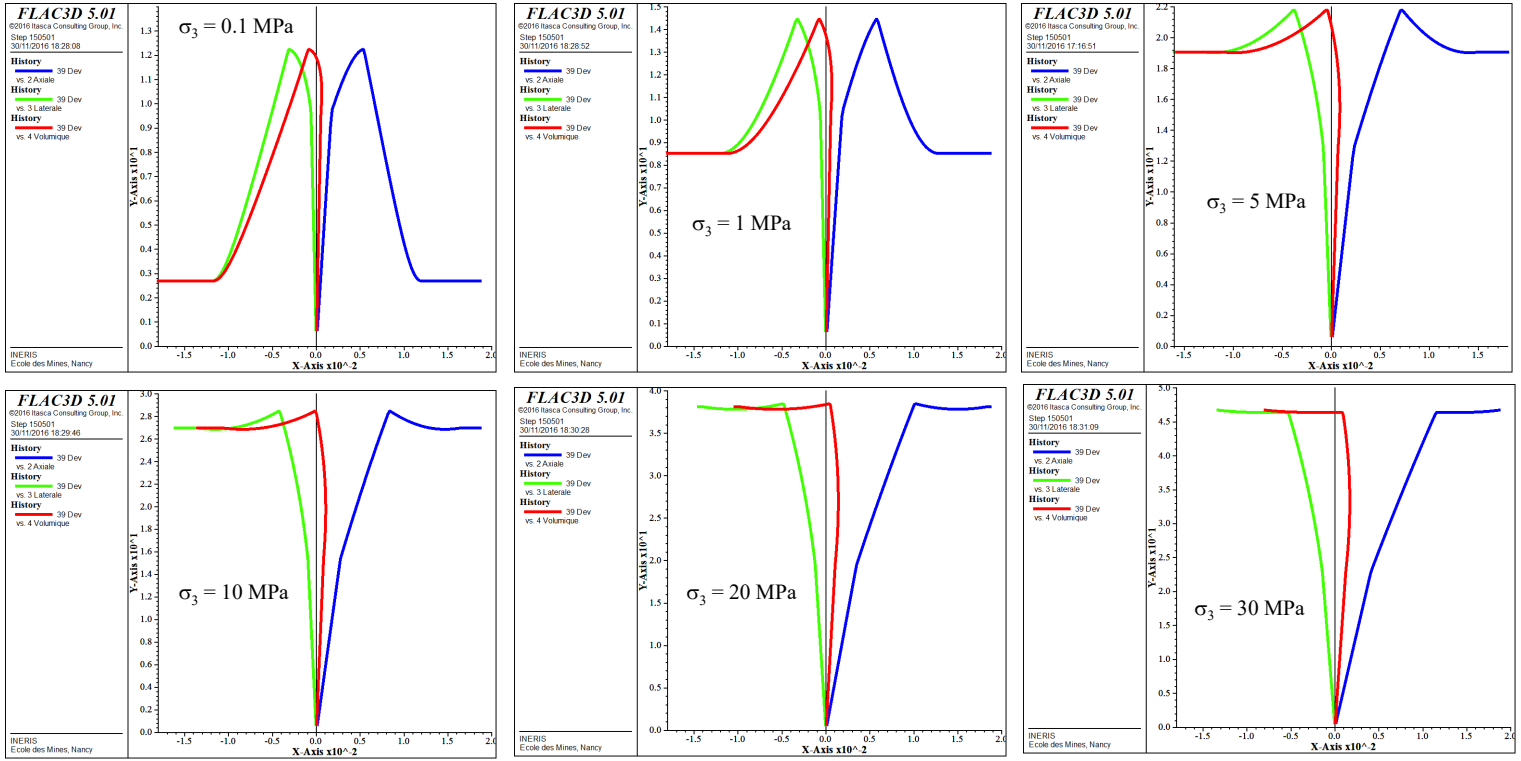

Simulation triaxial test (WP=0)

Yield functions: theoretical vs numerical solutions

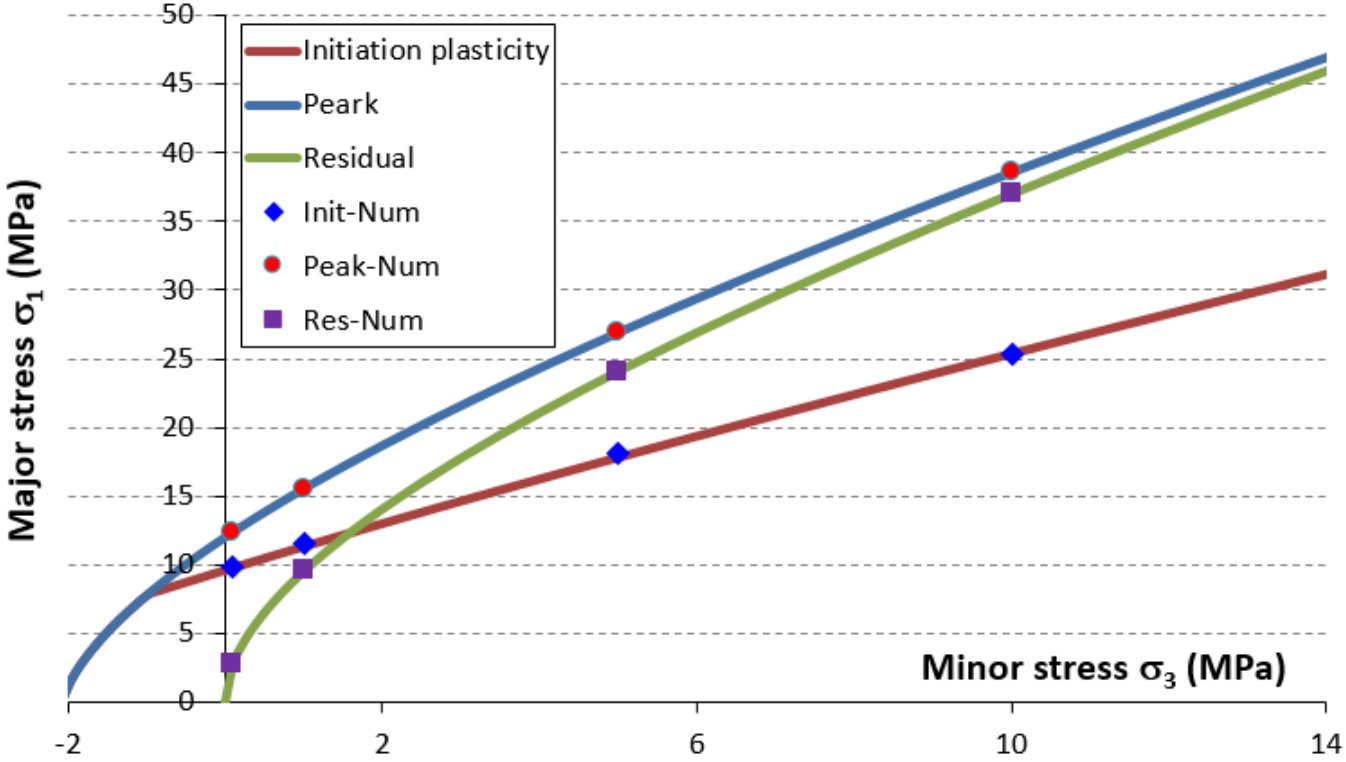

Simulation triaxial test with WP

Stress-strain curves

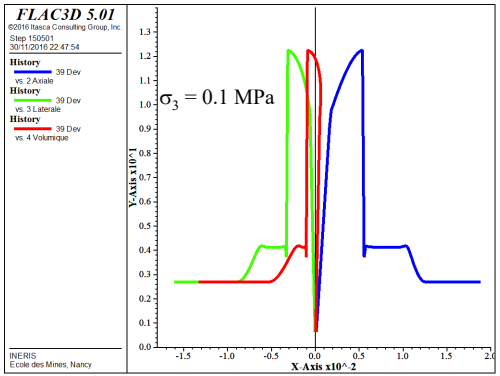

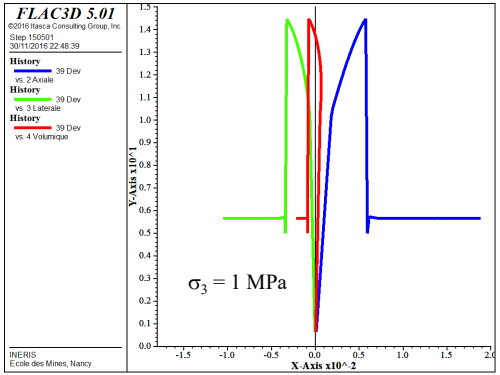

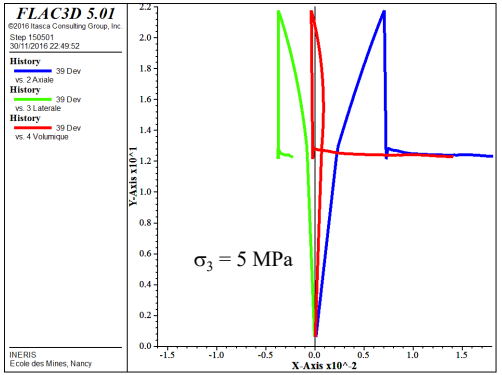

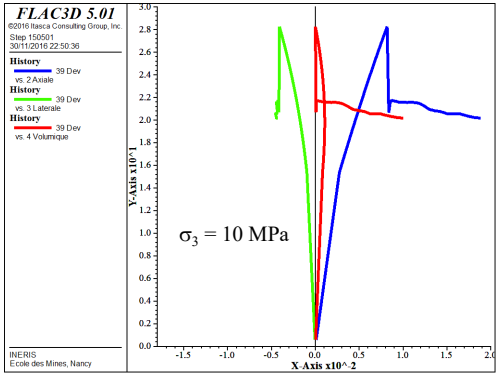

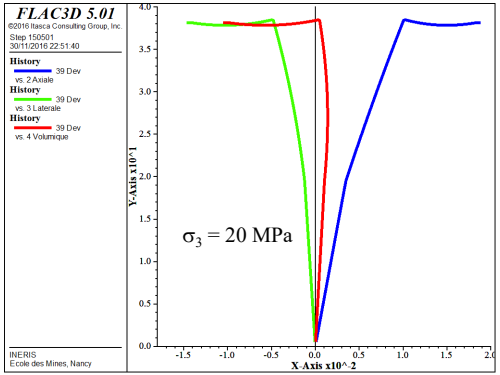

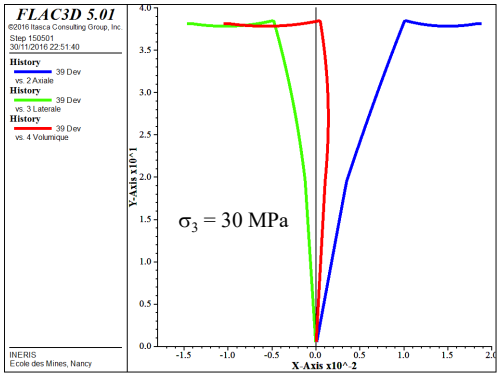

3D Simulation of structures

Numerical model

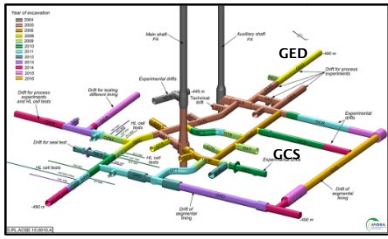

- Two drifts at the main level of Andra URL (-490 m): GCS and GED
  - In situ stresses: σ_H =16.1 MPa, σ_h = 12.4 MPa σ_v = 12.7 MPa (Armand et al 2017)
  - Drifts' circular section: radius 2.6 m; length 32 m
  - GCS//σ_H and GED//σ_h
  - 32 steps of excavation

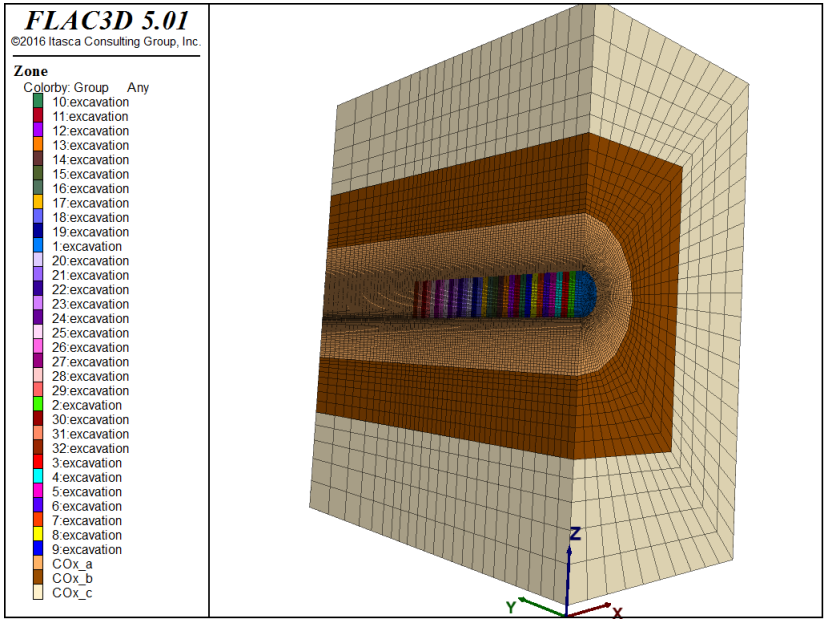

3D Simulation of structures

GCS drift // σ_H : Fractured zones

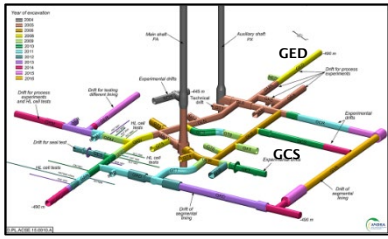

- 3D character
  - distribution of fractured zone varies from one section to another
  - fractures occur behind the front
- Two distint zones: connected (EDZ) and discrete (EdZ) fracture zones
- Good aggrement with in-situ observation in fractured zones' extension
  - Armand et al (2014): Horizontal extensions EDZ = 0.15xD to 0.5xD, EdZ = 0.5xD to 1xD

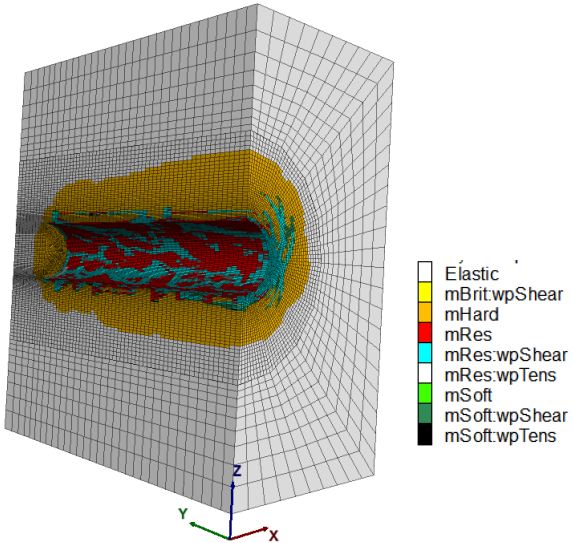

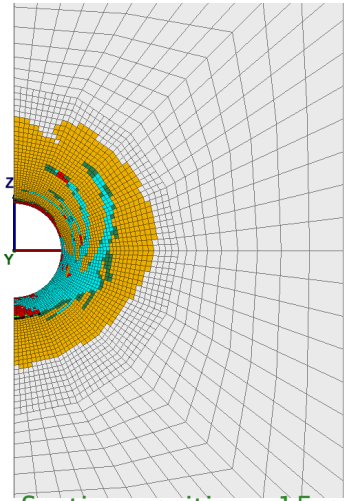

Section position : 15 m

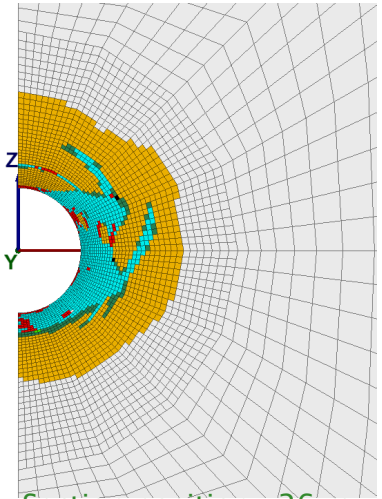

Section position : 26 m

3D Simulation of structures

GCS drift // σ_H : Convergences

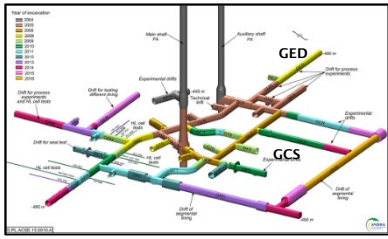

- 3D character
  - Instantaneous convergence varies from one section to another
- Magnitude and ratio of convergences (Ch/Cv~2) is in a good agreement with
  - In-situ observation (Armand et al 2013)
  - Empirical model (Guayacan-Carrillo et al 2017)

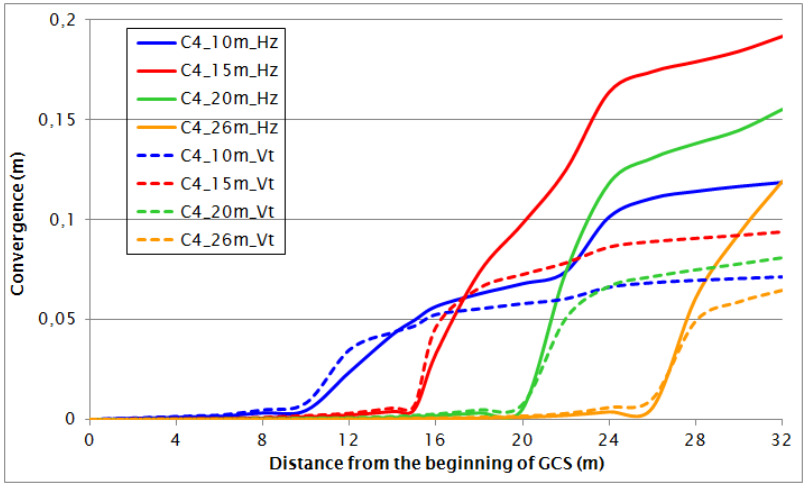

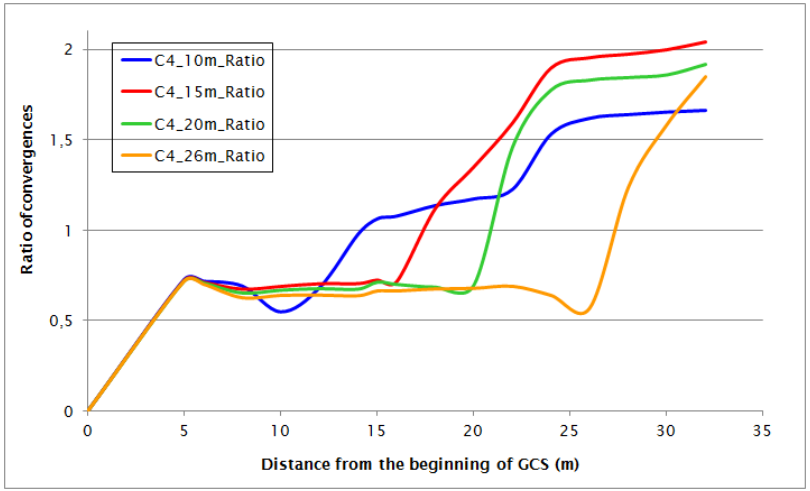

3D Simulation of structures

GED drift // σ_h : Fractured zones

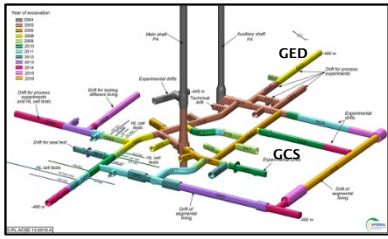

- 3D character
  - distribution of fractured zone varies from one section to another section
  - fractures occur behind the front
- Two distint zones: connected (EDZ) and discrete (EdZ) fracture zones
- Good aggrement with in-situ observation in fractured zones' extension
  - Armand et al (2014): Vertical extensions EDZ = 0.2xD to 0.5xD, EdZ = 0.6xD to 1.1xD

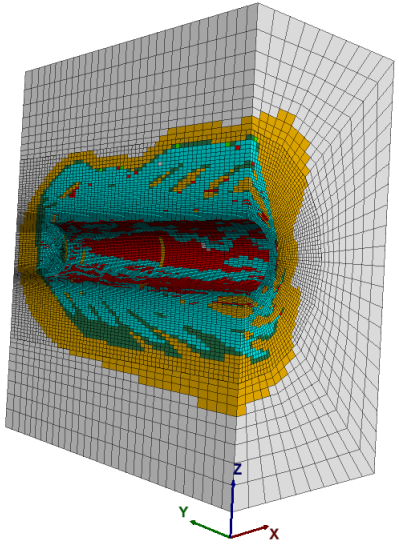

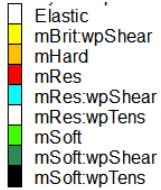

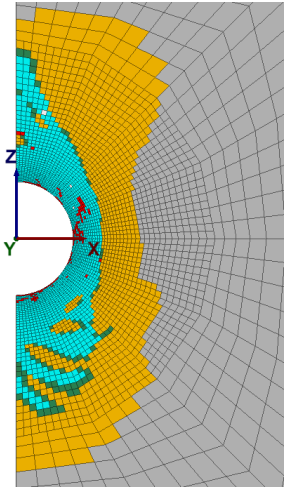

Section position : 15 m

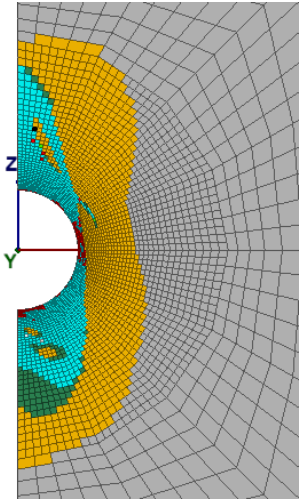

Section position : 26 m

3D Simulation of structures

GED drift // σ_h : Convergences

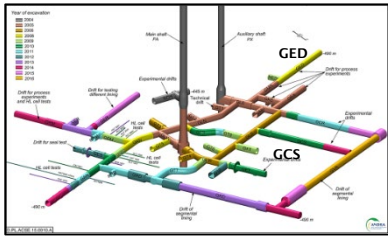

- 3D character
  - Instantaneous convergence varies from one section to another
- Magnitude and ratio of convergences (Ch/Cv~3-4) is in a good agreement with
  - In-situ observation (Armand et al 2013)
  - Empirical model (Guayacan-Carrillo et al 2017)

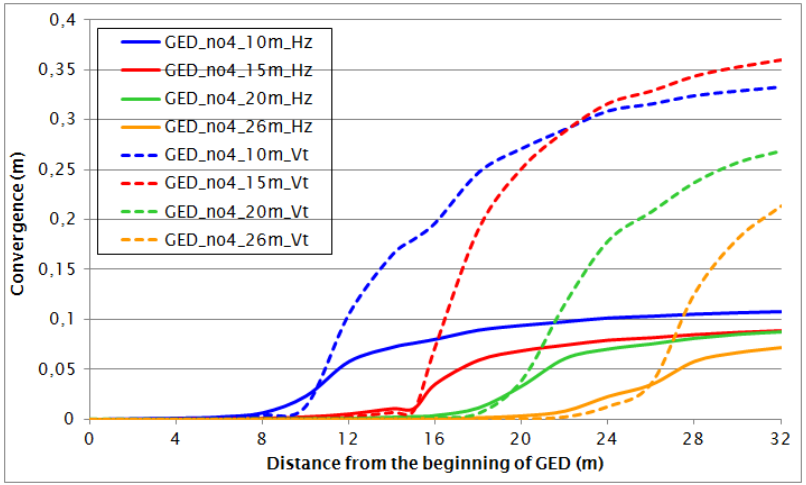

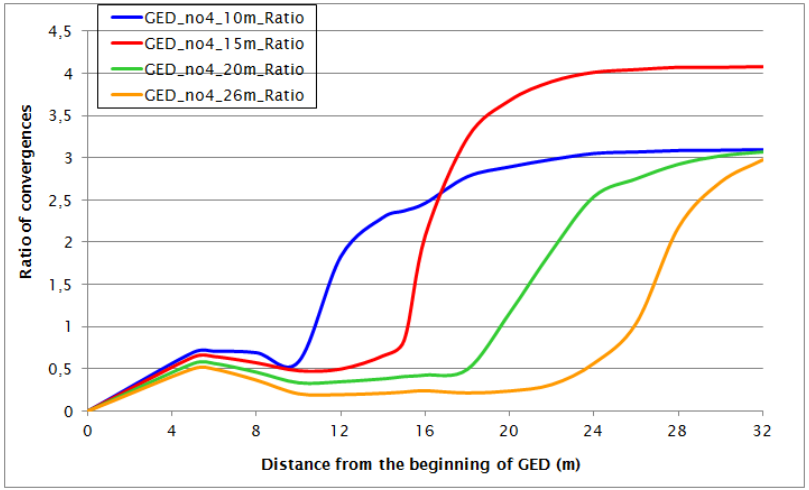

Conclusions

Induced anisotropy represented by

- Elasto-plastic rock matrix
- Weakness planes (ubiquitous joints) occuring during the post-peak stage
  - Their orientation depends on stress state

Application of the proposed model to describe the 3D excavation of two drifts GCS ($//\sigma_H$) and GED ($//\sigma_h$) in Andra URL

- 3D charaters of excavation induced damage zone and of deformation
- A good agreement with in-situ observations and emperical prediction

First 3D phenomenological model dedicated to both drifts GCS and GED

Further developements (already done)

- Hydromechanical coupling
- Time-dependent behavior
  - Rock matrix (Souley et al 2017)
  - Weakness plane

References

G Armand, F Leveau, C Nussbaum, R de La Vaissiere, A Noiret, D Jaeggi, P Landrein, C Righini (2014). Geometry and properties of the excavation induced fractures at the Meuse/Haute-Marne URL drifts. *Rock Mech. Rock Eng. ; 47: 21-41*

G Armand, F Bumbieler, N Conil, R de La Vaissière, KM Bosgiraud, MN Vu (2017), Main outcomes from in situ THM experiments programme to demonstrate feasibility of radioactive HL-ILW disposal in the Callovo-Oxfordian claystone, *Journal of Rock Mechanics and Geotechnical Engineering*, 9(3), 415-427.

G Armand, A Noiret, J Zghondi, DM Seyedi (2013). Short-and long-term behaviors of drifts in the Callovo-Oxfordian claystone at the Meuse/Haute-Marne Underground Research Laboratory. *Journal of Rock Mechanics and Geotechnical Engineering* 5 (3), 221-230

G Armand, N Conil, J Talandier, DM Seyedi (2017). Fundamental aspects of the hydromechanical behaviour of Callovo-Oxfordian claystone: from experimental studies to model calibration and validation. *Computers and Geotechnics* 85, 277-286

LM Guayacan-Carillo, J Sulem, DM Seyedi, S Ghabezloo, A Noire, G Armand (2015). Analysis of Long-Term Anisotropic Convergence in Drifts Excavated in Callovo-Oxfordian Claystone. *Rock mechanics and rock engineering* 45(1):97-114

MA Mánica, A Gens, J Vaunat, DF Ruiz (2018). Nonlocal plasticity modelling of strain localisation in stiff clays. *Computers and Geotechnics* 103, 138-150

M Souley, G Armand, JB Kazmierczak (2017). Hydro-elasto-viscoplastic modeling of a drift at the Meuse/Haute-Marne underground research laboratoratory (URL). *Computers and Geotechnics* 85, 306-320

C Yao, JF Shao, QH Jiang, CB Zhou (2017). Numerical study of excavation induced fractures using an extended rigid block spring method. *Computers and Geotechnics* 85, 368-383